

# An estimate of the time variation of the abundance gradient from planetary nebulae<sup>\*</sup>

## II. Comparison with open clusters, cepheids and young objects

W. J. Maciel, L. G. Lago, and R. D. D. Costa

Instituto de Astronomia, Geofísica e Ciências Atmosféricas (IAG), Universidade de São Paulo, Rua do Matão 1226, 05508-900 São Paulo SP, Brazil  
e-mail: [maciel;leonardo;roberto]@astro.iag.usp.br

Received 13 October 2004 / Accepted 18 November 2004

**Abstract.** The temporal behaviour of the radial abundance gradients has important consequences for models of the chemical evolution of the Galaxy. We present a comparison of the time variation of the abundance gradients in the Milky Way disk as determined from a sample of planetary nebulae, open clusters, cepheids and young objects, such as stars in OB associations and HII regions. We conclude that the [Fe/H] gradients as measured in open cluster stars strongly support the time flattening of the abundance gradient as determined from O/H and S/H measurements in planetary nebulae. This conclusion is also supported by the cepheid variables, for which very accurate gradients and ages can be determined, and also by some recent estimates for OB stars and HII regions. It is estimated that the average flattening rate for the last 8 Gyr is in the range 0.005–0.010 dex kpc<sup>-1</sup> Gyr<sup>-1</sup>.

**Key words.** planetary nebulae: general – ISM: abundances – Galaxy: abundances – open clusters and associations: general – Galaxy: disk

### 1. Introduction

It is now generally accepted that the radial abundance gradients observed in the Milky Way disk are among the main constraints of models of the chemical evolution of the Galaxy. The study of the gradients comprises the determination of their magnitudes along the disk, which include possible space variations, and their time evolution during the lifetime of the Galaxy (see for example Henry & Worthey 1999; Maciel 2000; and Maciel & Costa 2003, for recent reviews).

The magnitudes of the gradients can be derived from a variety of objects, such as HII regions, early type stars, planetary nebulae, open clusters etc. Recent investigations include Deharveng et al. (2000), Andrievsky et al. (2004), Friel et al. (2002) and Maciel et al. (2003), for HII regions, cepheid variables, open clusters and planetary nebulae, respectively. Average values are generally in the range –0.04 to –0.10 dex/kpc for the best observed element ratios, which are O/H and S/H in photoionized nebulae and Fe/H in stars.

The space variations of the gradients are more controversial. Some flattening at large galactocentric distances is clearly discernible in a sample of galactic planetary nebulae, as shown by Maciel & Quireza (1999) and more recently by

Costa et al. (2004), on the basis of a study of nebulae located in the direction of the galactic anticentre. These results are supported by some work on HII regions (see for example Vílchez & Esteban 1996). The cepheid data are consistent with a flattened gradient near the solar neighbourhood, as suggested by Andrievsky et al. (2004). On the other hand, no flattening has been observed in some recent studies of O, B stars in the galactic disk (see for example Smartt 2000) or from planetary nebulae (Henry et al. 2004), although in the latter case generally flatter gradients have been determined.

Probably the most interesting property of the gradients is their time evolution, as it appears to be a very distinctive constraint of many recent chemical evolution models (cf. Tosi 2000). As an example, models by Hou et al. (2000) and Alibés et al. (2001) predict a continuous time flattening of the gradients, while models by Chiappini et al. (2001) are consistent with some steepening on a timescale of 3 to 10 Gyr. Therefore, it is extremely important to obtain observational constraints on the time evolution of the gradients, along with their magnitudes and possible space variations. Recently, Maciel et al. (2003, hereafter referred to as Paper I) suggested that the O/H gradient has been flattening from roughly –0.11 dex/kpc to –0.06 dex/kpc during the last 9 Gyr, or from –0.08 dex/kpc to –0.06 dex/kpc in the last 5 Gyr. These results were obtained using a large sample of planetary nebulae for which accurate

<sup>\*</sup> Based on observations made at the European Southern Observatory (Chile) and Laboratório Nacional de Astrofísica (Brazil).

abundances are available, and for which the ages of the progenitor stars have been individually determined. As discussed by Maciel et al. (2003), the absolute ages derived are probably not accurate, but the relative ages of the stars are better determined, so that the time behaviour of the gradient can be derived, at least for the last 5 Gyr, which include most objects in the sample.

Along with planetary nebulae, open clusters are favorite objects to study the time evolution of abundance gradients, as they comprise a wide age bracket and have relatively well determined ages, based on detailed comparisons of theoretical isochrones and color magnitude diagrams (see for example Friel 1995, 1999; and Phelps 2000, for recent reviews). The distances are also generally well determined, while the stellar metallicities, mostly derived by photometric techniques, are not as accurate as in the case of some elements in photoionized nebulae, but nevertheless the gradients can be derived within a similar uncertainty, roughly 0.01 dex/kpc.

Cepheid variables are also very interesting objects to study abundance gradients, since their distances, ages and chemical composition can be extremely well determined in comparison with the other objects considered here. This can be observed in the recent series of papers by Andrievsky and collaborators (Andrievsky et al. 2002a,b,c, 2004; Luck et al. 2003). Cepheid variables are young objects spanning a limited range in ages, and we will show in Sect. 4 that this characteristic is crucial in the determination of the gradient at the present time.

In the present work, we take into account the results of Maciel et al. (2003, Paper I) and extend the discussion on the abundance gradients by (i) including S/H data as a tool in the study of the time variation of the gradients; (ii) adopting  $[\text{Fe}/\text{H}] \times \text{O}/\text{H}$  and S/H conversions based on our previous work; and (iii) making a detailed estimate of the gradient from Cepheid data and of the Cepheid age distribution. Finally, (iv) we take into account some recent determinations of the gradients from young objects, such as HII regions and stars in OB associations, and show that a detailed comparison of results based on samples of different objects, involving different techniques and observational data, leads to a consistent interpretation of the time variation of the radial abundance gradients in the galactic disk.

## 2. Gradients from planetary nebulae

### 2.1. O/H gradients

An estimate of the time variation of the O/H radial gradient in the galactic disk has recently been made by Maciel et al. (2003). From the observed O/H abundances in a large sample of nebulae, the  $[\text{Fe}/\text{H}]$  metallicity was determined on the basis of a correlation with  $[\text{O}/\text{H}]$  abundances derived for disk stars. Here the brackets refer to abundances relative to the Sun, as usual. An age-metallicity relation was used to estimate the ages of the progenitor stars, so that the temporal behaviour of the gradients could be derived. Two cases were considered (A and B), in which the sample was divided into three age groups, namely, Case A: Group I, with ages in the range  $0 < t(\text{Gyr}) < 3$ , Group II, for which  $3 < t(\text{Gyr}) < 6$ , and Group III, with

$t > 6$  Gyr; and Case B: Group I, with ages in the range  $0 < t(\text{Gyr}) < 4$ , Group II, for which  $4 < t(\text{Gyr}) < 5$ , and Group III, with  $t > 5$  Gyr.

The results of case B, which are statistically more significant, are shown in Table 1. The table gives the results for the O/H gradients in the form  $\log(\text{O}/\text{H}) + 12 = a + bR$ , where  $R$  is the galactocentric distance (kpc). The age groups are defined in Cols. 1 and 2, and we have adopted 8 Gyr as the upper age limit of the oldest group, since about 97% of the objects in our sample have ages lower than this limit. For each age group, the columns give the intercept  $a$  with associated uncertainties (Col. 3), the gradient  $b$  (dex/kpc) (Col. 4), the correlation coefficient  $r$  and number of data points  $n$  (Cols. 5 and 6, respectively). These gradients, as well as other gradients derived in this paper, were calculated adopting a value  $R_0 = 8.0$  kpc for the solar galactocentric distance. Recent discussions on this topic suggest  $R_0$  values in the range 7.6–8.0 kpc (see for example Reid 1993; Maciel 1993; McNamara et al. 2000). The adoption of different values within this range would have a small effect on the gradients, so that our results can be safely compared with other calculations using  $R_0 = 7.6$  kpc (Maciel & Quireza 1999) or  $R_0 = 7.9$  kpc (Andrievsky et al. 2004; Daflon & Cunha 2004, see Sects. 4 and 5).

The first three rows of Table 1 show that the O/H gradient flattens out in time, that is, the O/H gradient becomes steeper along the sequence of groups I, II and III. In this section, we will show that the observed flattening of the gradients does not depend on the precise definition of the age groups, which is largely arbitrary. To do this, we have divided the PN sample into two age groups only, which we will call Group I, or “younger”, and Group II, or “older”. Let  $t_1$  be the upper age limit of Group I, so that all PN progenitors having ages  $t \leq t_1$  will belong to Group I, while those with ages  $t > t_1$  belong to Group II. We have then adopted several different values of  $t_1$  in the range  $3.0 < t_1(\text{Gyr}) < 6.0$ , and for each of these values we have calculated the O/H gradient of the corresponding Groups I and II.

Figure 1 shows the obtained O/H gradients as a function of the age limit  $t_1$ . The gradients of Group I are shown as empty circles connected by lines, while those of Group II are represented by filled circles. From this figure, it becomes immediately clear that the younger Group I has systematically flatter gradients than the older Group II, irrespective of the adopted age limit, that is, the O/H gradient appears to be flattening out in time, no matter how one defines Groups I and II. It can also be seen that the difference between the gradients of Groups I and II increases with  $t_1$ , which reflects the fact that for larger  $t_1$  values only the oldest objects, which show the steepest gradients, are allocated to Group II.

Naturally, for values of  $t_1$  close to the minimum age limit,  $t_1 \simeq 3$  in Fig. 1, most objects are allocated to Group II, so that Group I becomes too small. Conversely, for  $t_1 \simeq 6$  most objects are in Group I, and Group II becomes underpopulated. Therefore, in these cases the correlation is less meaningful, so that the best results are obtained for  $t_1 \simeq 4$  to 5 Gyr, approximately.

From the results in Fig. 1 and Table 1, it can be seen that the O/H gradient flattens out from the older groups to the younger

**Table 1.** Abundance gradients from planetary nebulae, given as  $\log(X/H) + 12 = a + bR$ .

Group	Age (Gyr)	$a$	$b$ (dex/kpc)	$r$	$n$	$d[\text{Fe}/\text{H}]/dR$
O/H gradients						
I	0–4	$9.252 \pm 0.064$	$-0.047 \pm 0.007$	-0.64	66	$-0.056 \pm 0.008$
II	4–5	$9.337 \pm 0.027$	$-0.089 \pm 0.003$	-0.94	99	$-0.107 \pm 0.004$
III	5–8	$9.049 \pm 0.072$	$-0.094 \pm 0.010$	-0.75	69	$-0.113 \pm 0.012$
S/H gradients						
I	0–4	$7.648 \pm 0.132$	$-0.080 \pm 0.014$	-0.66	44	$-0.096 \pm 0.017$
II	4–8	$7.730 \pm 0.091$	$-0.113 \pm 0.011$	-0.76	72	$-0.136 \pm 0.013$

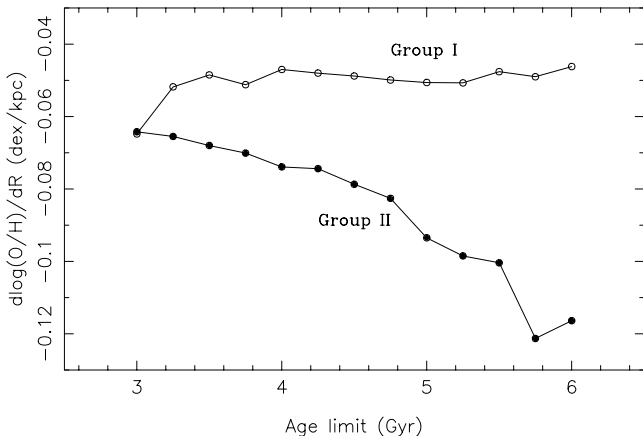


**Fig. 1.** Time variation of the O/H gradient from planetary nebulae. The PN sample was divided into two age groups, Group I (“younger”), with ages lower than the age limit  $t_1$ , and Group II (“older”), with ages higher than  $t_1$ . The plot shows the O/H gradient (dex/kpc) of each group as a function of the upper age limit of Group I,  $t_1$ . The gradients of the younger Group I (open circles connected by lines) are always flatter than those of the older Group II (filled circles connected by lines). The best results apply for  $t_1 \simeq 4$  to 5 Gyr, approximately, for which the correlations are more meaningful.

ones. Although the choice of the age groups is arbitrary, in all cases considered by us the flattening of the gradient is apparent. As discussed by Maciel et al. (2003), even though the *absolute* ages may be in error, it is unlikely that the *relative* ages are incorrect, so that the flattening of the gradients is probably real. Also, by considering two age groups only, the probability of placing a given object in the wrong group is relatively small. Furthermore, Maciel et al. (2003) performed an independent calculation of the ages, on the basis of a relationship between the N/O abundance and the progenitor star mass, which led to the original stellar mass on the main sequence and therefore to another estimate of the age, with results similar to those shown in Table 1.

In order to compare the PN derived gradients with results from other objects, especially open cluster stars and cepheids, it is interesting to convert the observed O/H gradient into [Fe/H] gradients. In fact, the O/H and [Fe/H] are expected to be similar, but not identical, which can be concluded by an inspection of the relation between the [O/Fe] ratio and the metallicity [Fe/H] in the galactic disk (see for example the

discussion by Maciel 2002). [Fe/H] gradients cannot be determined directly from planetary nebulae, as the iron lines are weak and a sizable fraction of this element is probably locked up in grains. However, a relation between the iron and oxygen abundances can be derived from observed properties of the stellar populations in the galactic disk. A detailed discussion on the metallicities and radial gradients from a variety of sources such as HII regions, hot stars and planetary nebulae in the galactic disk has been recently presented by Maciel (2002). According to this analysis, an independent [O/Fe]  $\times$  [Fe/H] relation has been obtained for the galactic disk, from which we can write approximately

$$[\text{Fe}/\text{H}] = \gamma + \delta (\log \text{O}/\text{H} + 12), \quad (1)$$

where  $\gamma$  and  $\delta$  are coefficients essentially independent of the galactocentric distance. An average value  $\delta \simeq 1.2$  was determined by Maciel (2002), which is slightly lower than the value adopted for the solar neighbourhood by Maciel et al. (2003),  $\delta \simeq 1.4$ . In fact, this parameter may show some time dependence, as we will see from a comparison of the PN gradients with those derived from open clusters, but it is typically in the range  $\delta \simeq 1.0$ –1.5, so that the main conclusions of this paper are not affected by this variation. Since both O/H and [Fe/H] gradients are assumed to be linear, it is easy to see that

$$\frac{d[\text{Fe}/\text{H}]}{dR} \simeq \delta \frac{d \log (\text{O}/\text{H})}{dR}, \quad (2)$$

which can be applied to the O/H gradients of Table 1. The derived [Fe/H] gradients are given in the last column of Table 1.

It should be mentioned that we have taken into account the new determinations of the solar oxygen abundance, which has been revised downwards following new 3D model atmospheres (Allende-Prieto et al. 2001; Asplund 2003; Asplund et al. 2004). We have adopted here  $\log (\text{O}/\text{H})_{\odot} + 12 = 8.7$ .

## 2.2. S/H gradients

Radial gradients involving the S/H ratio can also be derived from planetary nebulae, as shown for example in our earlier work (Maciel & Köppen 1994; Maciel & Quireza 1999), as well from HII regions (see for example Afflerbach et al. 1997). The obtained values are similar and probably slightly steeper than the O/H gradient.

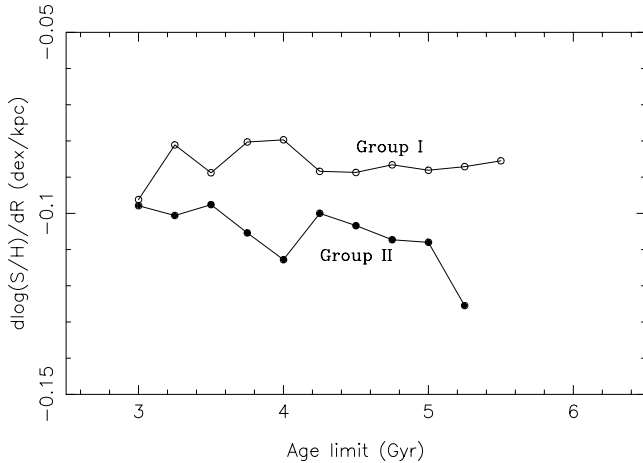


**Fig. 2.** The S/H gradient (dex/kpc) from planetary nebulae, divided into two age groups, as a function of the upper age limit of Group I. The gradients of the younger Group I (open circles connected by lines) are always flatter than those of the older Group II (filled circles connected by lines).

We have considered the objects in the sample of Maciel et al. (2003) for which reliable sulfur data are available and applied the same procedure as for the O/H ratio. Lists of objects and corresponding abundances are given in Maciel & Quireza (1999) and Maciel et al. (2003), which were supplemented by the new results for anticentre nebulae by Costa et al. (2004). In view of the weakness of the sulfur lines in photoionized nebulae, and the possible effect of the  $S^{+++}$  ion (see Henry et al. 2004, for a discussion), the derived abundances are somewhat less accurate than for oxygen, which is reflected by a smaller sample and a relatively larger dispersion. For this reason, we decided to divide the PN sample into two age groups only, namely Groups I and II, which we will refer to as the “younger” and “older” groups, respectively. This is basically the same procedure adopted in the previous sub-section, which led to Fig. 1. Since all objects in our sample have ages lower than 7 Gyr, we have adopted several values for the upper age limit of the younger group in the range  $3.0 < t_1$  (Gyr)  $< 6.0$ .

Figure 2 shows the derived S/H gradients as a function of the upper age limit for Group I, and can be compared with Fig. 1. It can be seen that the younger group I (empty circles) shows gradients systematically flatter than the older Group II (filled circles), in agreement with the results for oxygen. Again, for  $t_1 \leq 3$  Gyr and  $t_1 \approx 6$  Gyr the samples become too small, and no meaningful results can be obtained, so that the best results occur for ages in the range  $3.5 < t_1$  (Gyr)  $< 5$ . As an example, Fig. 3 shows the derived gradients for the case  $t_1 = 4.0$  Gyr, that is, in this case the objects in the younger Group I have ages lower than 4 Gyr, while the older group II has ages larger than 4 Gyr. The corresponding values are given in the last two rows of Table 1 for the two age groups. Again the flattening of the gradients with time is apparent.

In order to convert the S/H gradients into [Fe/H] gradients, we have followed the same procedure as for oxygen, and have first obtained a correlation between the S/H and O/H abundance ratios. Such a correlation is predicted by nucleosynthetic

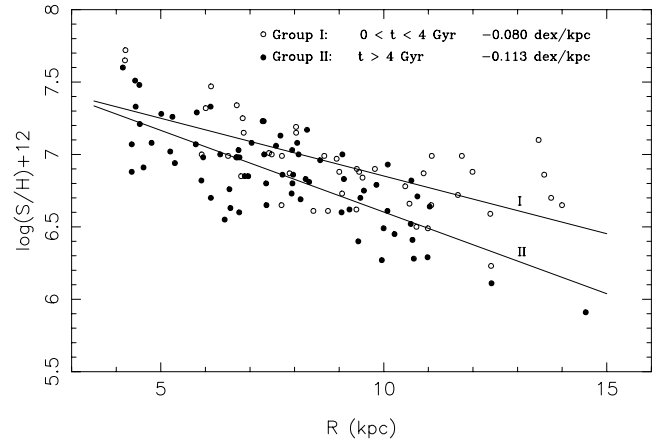


**Fig. 3.** The S/H abundance gradient from planetary nebulae, divided into two age groups: Group I ( $t < 4$  Gyr, empty circles) and Group II ( $t > 4$  Gyr, filled circles). The corresponding gradients (dex/kpc) are shown in the figure. The adopted value of the galactocentric distance of the Sun is  $R_0 = 8.0$  kpc.

models of intermediate mass stars, since S and O are not basically altered by the evolution of the progenitor stars of planetary nebulae. In fact, several people have independently obtained relatively tight correlations between S/H and O/H, as well as for Ne/H and Ar/H (see for example Köppen et al. 1991; Maciel & Köppen 1994; Costa et al. 2004; Henry et al. 2004). From these references, and especially from the results of our own group (Maciel & Köppen 1994; Maciel & Quireza 1999; Costa et al. 2004), we conclude that the slope is very close to unity, so that we can apply for the S/H gradient the same correction factor as for O/H, namely,  $d[\text{Fe}/\text{H}]/dR \approx 1.2 d \log(\text{S}/\text{H})/dR$ . The corresponding [Fe/H] gradients are also given in the last column of Table 1.

### 3. Gradients from open clusters

As mentioned in the Introduction, open clusters are favorite objects for which the determination of abundance gradients is possible (Janes 1979; Friel 1995; Phelps 2000). In a recent work, Friel and collaborators presented a sample of 39 open clusters for which metallicities, distances and ages have been determined in a homogeneous and consistent way (Friel et al. 2002, see also Friel 2005). On the basis of a updated abundance calibration of spectroscopic indices in a sample containing 459 stars, Friel et al. (2002) derived an average [Fe/H] gradient of  $-0.06$  dex/kpc in a range of galactocentric distances of 7 to 16 kpc. Taking into account age groups defined in several different ways, they concluded that there is an indication of some time flattening of the gradients. For example, for clusters with ages under 2 Gyr, the derived gradient is  $-0.023$  dex/kpc; for ages between 2 Gyr and 4 Gyr, the gradient is  $-0.053$  dex/kpc, and for those older than 4 Gyr they obtained  $-0.075$  dex/kpc.

More recently, new catalogues and compilations of open clusters have become available (Chen et al. 2003; Dias et al. 2002), which include space and kinematical data, as well as metallicities and estimates of the ages. Chen et al. (2003)

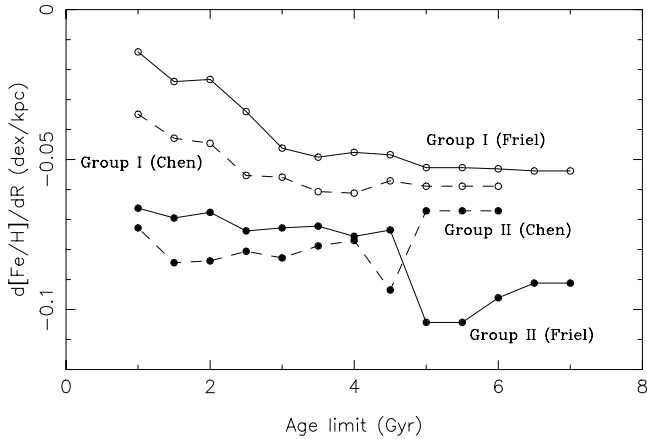


**Fig. 4.** The  $[\text{Fe}/\text{H}]$  gradient (dex/kpc) from the samples of open clusters by Friel et al. (2002, solid lines), and Chen et al. (2003, dashed lines), divided into two age groups, as a function of the upper age limit of Group I. As for the case of planetary nebulae, the gradients of the younger Group I (open circles) are always flatter than those of the older Group II (filled circles).

assembled a total of 119 clusters, for which distances and metallicities are available, which led to an average gradient of  $d[\text{Fe}/\text{H}]/dR \approx -0.063$  dex/kpc for the whole sample, similar to the value derived for the homogeneous sample by Friel et al. (2002). Taking into account two different age groups (ages  $<0.8$  Gyr and  $\geq 0.8$  Gyr, respectively), Chen et al. (2003) concluded that the iron gradient was steeper in the past, supporting the earlier conclusion by Friel et al. (2002).

In order to obtain a more accurate comparison between the  $[\text{Fe}/\text{H}]$  gradients from open clusters and the planetary nebula data, we have used both the homogeneous sample by Friel et al. (2002) and the compilation by Chen et al. (2003) and rederived the  $[\text{Fe}/\text{H}]$  gradients, taking into account several possibilities of defining the age groups. Following the same procedure as for the O/H and S/H gradients in planetary nebulae, we have divided the open cluster stars into two age groups, varying the upper age limit of the younger Group I.

Figure 4 shows the  $[\text{Fe}/\text{H}]$  gradient as a function of the upper age limit of Group I for the samples of Friel et al. (2002, solid lines) and Chen et al. (2003, dashed lines). Again we observe the same behaviour as in Figs. 1 and 2, in the sense that the gradients of Group I objects are always flatter than for Group II. We can obtain a more detailed result dividing the open clusters into three age groups, as done by Chen et al. (2003). A representative example is given in Table 2, where the groups are defined in Cols. 1 and 2, and the parameters of the fits are shown in Cols. 3 to 6. The upper age limit is again 8 Gyr, which includes about 96% of the total sample of open clusters, in good agreement with the recent estimates for the ages of the oldest open clusters by Salaris et al. (2004). We have restricted our analysis to galactocentric distances  $R < 16$  kpc, and excluded the object Berkeley 29, which does not satisfy this criterium (see Chen et al. 2003, for details). The total number of clusters in the samples are 39 and 118 for the objects of Friel et al. (2002) and Chen et al. (2003), respectively. It should be noted that both samples are not completely independent, as

**Table 2.** Abundance gradients from open clusters, given as  $[\text{Fe}/\text{H}] = a + bR$ .

Group	Age (Gyr)	$a$	$b$ (dex/kpc)	$r$	$n$
Friel					
I	0–2	$-0.023 \pm 0.169$	$-0.023 \pm 0.019$	-0.33	15
II	2–5	$0.279 \pm 0.156$	$-0.058 \pm 0.014$	-0.77	14
III	5–8	$0.715 \pm 0.327$	$-0.104 \pm 0.035$	-0.73	10
Chen					
I	0–0.8	$0.185 \pm 0.103$	$-0.024 \pm 0.012$	-0.22	80
II	0.8–2	$0.467 \pm 0.175$	$-0.067 \pm 0.018$	-0.69	18
III	2–8	$0.681 \pm 0.218$	$-0.084 \pm 0.020$	-0.71	20

most of the objects in the Friel sample are also contained in the compilation by Chen et al. (2003), although the adopted parameters (ages and metallicities) are often different. However, the fact that the homogeneous sample by Friel et al. and the compilation by Chen et al. lead essentially to the same results shows that the lack of homogeneity in the determination of key parameters such as the ages and metallicities in the larger sample by Chen et al. does not introduce any significant uncertainty relative to the homogeneously obtained sample by Friel et al. (2002).

Taking into account the larger sample by Chen et al. (2003), we notice that most of the age groups have galactocentric distances roughly in the range  $R \approx 6$  to 15 kpc, which is wide enough so that the derived gradients are representative of the galactic disk. However, there is some tendency for the youngest clusters to be located at galactocentric distances closer than about 10 kpc, which probably reflects the fact that older clusters are destroyed by collisions with molecular clouds in the inner Galaxy. Therefore, the distribution of the young clusters presents a more limited range of galactocentric distances, so that the derived gradients may be artificially flat, which is also reflected by the lower correlation coefficients of Group I in both samples, as can be seen in Table 2. In order to investigate the amount by which this affects the results for the gradients at the present time, we will consider in the next section the abundance gradients as derived from cepheid variable stars.

## 4. Cepheid variables

### 4.1. The $[\text{Fe}/\text{H}]$ gradient from cepheids

Cepheid variables have a distinct role in the determination of radial abundance gradients and their time variations for a number of reasons. First, they are usually bright enough that they can be observed at large distances, providing accurate abundances; second, their distances are generally well determined, as these objects are often used as distance calibrators; third, their ages are also well determined, on the basis of relations involving their periods, luminosities, masses and ages. Of course, they generally have ages close to a few hundred million years, so that they cannot be used alone in the study of the time variations of the gradients, but define instead an accurate benchmark for the value of the gradient at their age bracket.

Recently, accurate abundances of several elements have been derived by Andrievsky et al. (2002a,b,c, 2004) and Luck et al. (2003) for a large sample of galactic cepheids. The total sample includes over 120 objects, and abundances of about 20 heavy elements have been derived, including C, O and Fe up to Nd and Eu. A clear negative gradient is evident from their results (see for example Fig. 3 of Andrievsky et al. 2004), which is roughly similar to the gradients derived from planetary nebulae and HII regions. Regarding the  $[\text{Fe}/\text{H}]$  abundances, which are better determined, they suggest a three zone gradient, amounting to  $d[\text{Fe}/\text{H}]/dR \approx -0.128$  dex/kpc for  $R = 4.0\text{--}6.6$  kpc (zone I);  $d[\text{Fe}/\text{H}]/dR \approx -0.044$  dex/kpc for  $R = 6.6\text{--}10.6$  kpc (zone II); and  $d[\text{Fe}/\text{H}]/dR \approx 0.004$  dex/kpc for  $R = 10.6\text{--}14.6$  kpc (zone III), where they have taken  $R_0 = 7.9$  kpc. A change of slope near the solar galactocentric radius has also been suggested by Caputo et al. (2001) for cepheids and Twarog et al. (1997) for open clusters. Also, the flattening of the gradient at large galactocentric distances is probably real, and has been observed by our group from planetary nebulae (cf. Costa et al. 2004; and Maciel & Quireza 1999). The division in three zones as adopted by Andrievsky et al. (2004) is based on a smoothing of the data, which makes no assumptions about the structure of the gradient. However, the three zones are not equally populated, zones I and III being undersampled relatively to zone II, which may affect the gradients. On the other hand, an average gradient valid for all zones can represent very well the cepheid data, as we will show, and is more adequate in order to make comparisons with other data.

We have taken into account the complete sample of Andrievsky et al. (2002a,b,c, 2004) and Luck et al. (2003) and rederived the  $[\text{Fe}/\text{H}]$  gradient adopting  $R_0 = 8.0$  kpc. We have obtained the following result:

$$[\text{Fe}/\text{H}] = 0.459 \pm 0.032 - (0.054 \pm 0.003) R \quad (3)$$

with a correlation coefficient  $r = -0.82$  and a total of  $n = 127$  stars. These results are shown in Fig. 5, again for  $R_0 = 8.0$  kpc, with no significant changes for  $7.6 < R_0(\text{kpc}) < 8.0$ . The derived gradient is also similar to the average value one would get combining the three zones considered by Andrievsky et al. (2004). It should be noted that the correlation shown by Fig. 5 is very well defined, as can be seen by the large correlation coefficient obtained, which also reflects the high accuracy of the spectroscopic cepheid data.

#### 4.2. Age distribution of cepheids

In order to compare the average gradients derived in the previous subsection with those from planetary nebulae and open cluster stars, it is necessary to estimate the age distribution of our sample of cepheid variables. We have accomplished that using two different methods, which we shall call Method 1 and Method 2. In both cases we have used the periods, effective temperatures and gravities given by Andrievsky et al. (2002a,b,c, 2004) and Luck et al. (2003). The main difference of the methods lies essentially in the determination of the stellar luminosities.

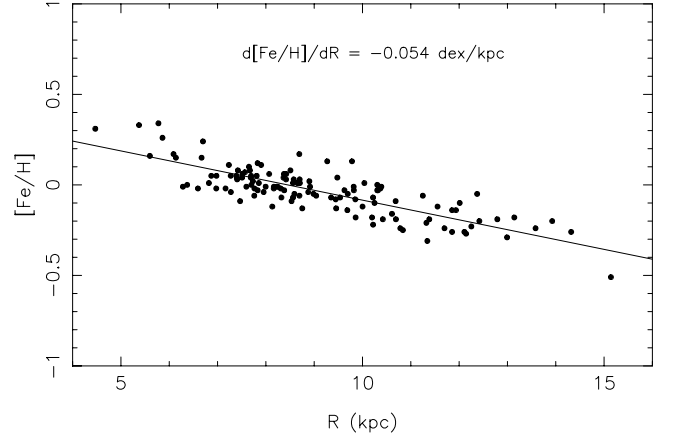


**Fig. 5.** The  $[\text{Fe}/\text{H}]$  abundance gradient from cepheid variable stars. The correlation coefficient is  $r = -0.82$ , and a total of 127 stars have been included. The adopted value for the galactocentric distance of the Sun is  $R_0 = 8.0$  kpc.

**Method 1** - We have first derived a very simple period-luminosity relation for galactic cepheids using data from Cox (2000), which can be written as

$$\log \frac{L_*}{L_\odot} = 2.291 + 1.266 \log P, \quad (4)$$

where the period  $P$  is in days. Since  $L_* = 4\pi R_*^2 \sigma T_{\text{eff}}^4$  and  $g = GM_*/R_*^2$ , where  $R_*$  and  $M_*$  are the stellar radius and mass, respectively, and  $T_{\text{eff}}$  is the effective temperature, the stellar mass can be derived for each object. The age follows from the calibration by Bahcall & Piran (1983) given by

$$\log t = 10 - 3.6 \log \frac{M_*}{M_\odot} + \left( \log \frac{M_*}{M_\odot} \right)^2, \quad (5)$$

where the age  $t$  is in yr. An alternative mass-age relationship can be obtained from Binney & Merrifield (1998, p. 280, Eqs. (5.5) and (5.6)), from which we have

$$\log t = 9.75 - 2.5 \log \frac{M_*}{M_\odot}, \quad (6)$$

which is valid for masses in the range  $2 < M_*/M_\odot < 20$ . Here again the age  $t$  is in yr.

**Method 2** - The second method uses the metallicity-dependent period-luminosity relation recently derived by Groenewegen et al. (2004), which can be written for galactic cepheids as

$$\log \frac{L_*}{L_\odot} = 2.432 + 1.092 \log P + 0.254 [\text{Fe}/\text{H}] - 0.4 BC. \quad (7)$$

The bolometric correction  $BC$  was approximated as a function of the effective temperature from Cox (2000) as

$$BC = a_1 + a_2 \log T_{\text{eff}} + a_3 (\log T_{\text{eff}})^2, \quad (8)$$

where  $a_1 = -899.14547$ ,  $a_2 = 477.87397$ ,  $a_3 = -63.48878$ . Once the stellar luminosity has been obtained, the same procedure as in method 1 is observed in order to derive the stellar ages.

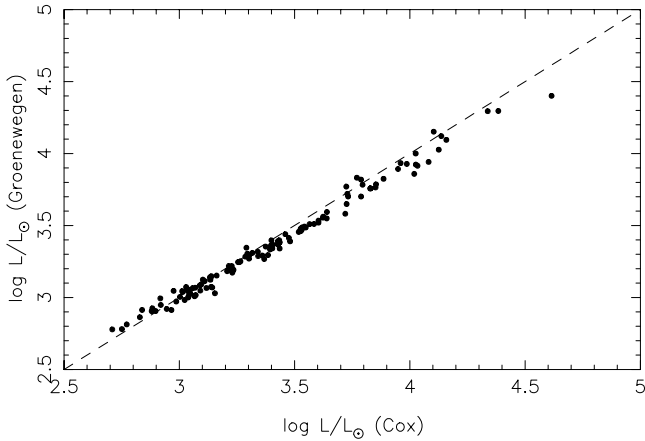


**Fig. 6.** A comparison of the luminosities calculated using Method 1 (Eq. (4)) from Cox (2000) and Method 2 (Eq. (7)) from Groenewegen et al. (2004).

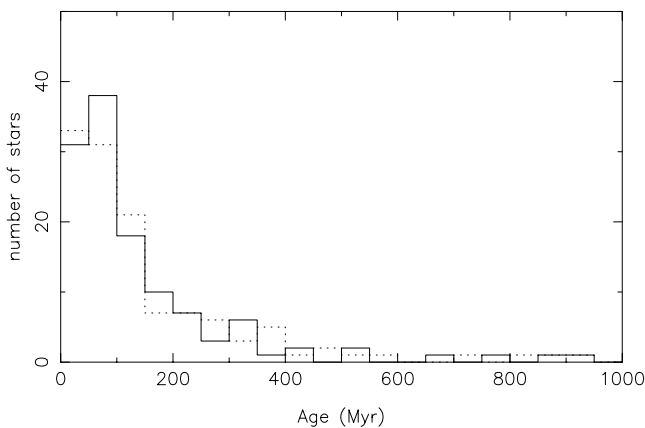


**Fig. 7.** A comparison of the age distributions of cepheid variables using ages from Bahcall & Piran (1983) (solid line, see Eq. (5)) and Binney & Merrifield (1998) (dotted line, see Eq. (6)). The period-luminosity relation is from Groenewegen et al. (2004), (see Eq. (7)).

A comparison of the luminosities derived from methods 1 and 2 for the stars in our sample is shown in Fig. 6. It can be seen that the agreement is very good, within 11% in average, so that the correction due to the metallicity effects is small for all stars in our sample.

The ages derived from methods 1 and 2 are then very similar, the average difference between them being less than 20% in all cases. This can be seen in the histograms shown in Fig. 7, where ages using Bahcall & Piran (1983, Eq. (5), solid line) or Binney & Merrifield (1998, Eq. (6), dotted line) have been used. The adopted period–luminosity relation is Eq. (7), from Groenewegen et al. (2004).

The maximum ages calculated from both methods for the stars in our sample is about 1 Gyr, but most objects are much younger, as can be seen from Fig. 7. In fact, about 80% of the stars have ages under 200 Myr, and 96% of the cepheids are younger than 700 Myr, so that the average gradient of the whole sample can be considered as representative of the “young objects”, as compared with most planetary nebulae and open cluster stars. In the following, we will then adopt a gradient of

$d[\text{Fe}/\text{H}]/dR = -0.054 \pm 0.003$  dex/kpc for cepheid variables in the approximate age range of 0 to 700 Myr.

## 5. Young objects

In order to obtain a comprehensive analysis of the time variation of the abundance gradients, it is interesting to take into account some very young objects, such as HII regions and OB stars in associations and young clusters, which better represent the youngest population for which meaningful gradients can be derived.

### 5.1. HII regions

HII regions are classic objects in the determination of abundance gradients, both in the Milky Way and in other galaxies (see for example Henry & Worthey 1999, for a recent review). Several people have derived O/H gradients from galactic HII regions (see for example Vilchez & Esteban 1996; Afflerbach et al. 1997; Deharveng et al. 2000; Pilyugin et al. 2003, for recent determinations). Generally, the most reliable determinations are those based on measured [OIII]  $\lambda 4959, 5007/4363$  lines, so that the electronic temperature can be derived. The average values of the O/H gradients are in the range  $-0.040$  to  $-0.070$  dex/kpc, the flatter end being preferred by the most recent papers of Deharveng et al. (2000) and Pilyugin et al. (2003). This derived range is considerably larger than the formal uncertainties of each determination, which is typically of the order of 0.005 dex/kpc. Therefore, we will adopt here a conservative average value given by  $d \log(\text{O}/\text{H})/dR \approx -0.055 \pm 0.015$  dex/kpc for the oxygen gradient from HII regions. In order to estimate the corresponding [Fe/H] gradient, we will adopt the same correction factor as for the planetary nebulae, so that we have  $d[\text{Fe}/\text{H}]/dR \approx -0.066 \pm 0.018$  dex/kpc. Since typical HII regions have ages in the Myr range, we may safely assume that they are representative of the present day gradients.

### 5.2. OB stars

A sample containing 69 stars in OB associations, open clusters and HII regions has been recently analysed by Daflon & Cunha (2004), on the basis of self-consistent non-LTE models with a homogeneous set of stellar parameters. Abundances of the elements C, N, O, Mg, Al, Si and S have been obtained, for which radial abundance gradients have been computed. The sample objects have generally well determined distances, and they are all young, with ages under 50 Myr, so that the derived gradients can also be considered as representative of the present day abundances in the galactic disk. The average gradient derived by Daflon & Cunha (2004) for all elements is  $-0.042 \pm 0.007$  dex/kpc adopting  $R_0 = 7.9$  kpc, which does not change for  $R_0 = 8.0$  kpc. For oxygen, they obtain a gradient of  $-0.031 \pm 0.012$  dex/kpc, so that applying the same correction factor of 1.2 as before, we obtain a gradient of  $d[\text{Fe}/\text{H}] = -0.037 \pm 0.014$  dex/kpc, which is very close to the average value derived by Daflon & Cunha (2004).

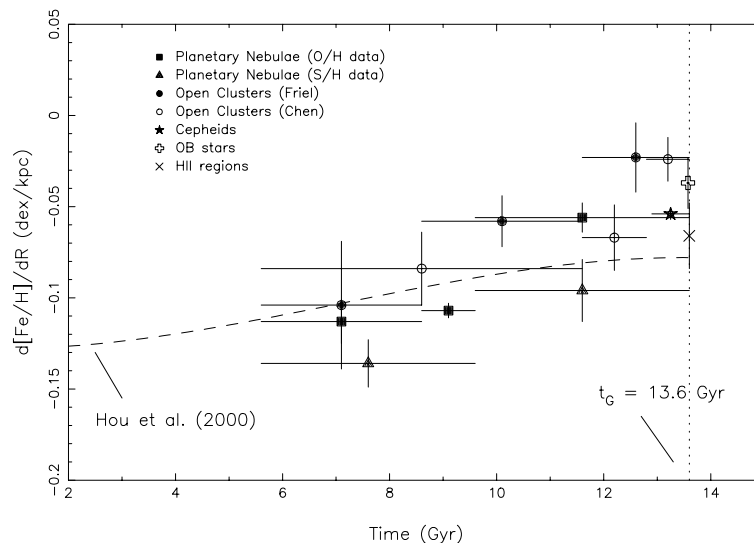


**Fig. 8.** Time variation of the  $[\text{Fe}/\text{H}]$  abundance gradient (dex/kpc). The converted  $[\text{Fe}/\text{H}]$  gradients from planetary nebulae are shown as filled squares (O/H data) and filled triangles (S/H data). The open cluster results are shown as filled circles (data from Friel et al. 2002) and empty circles (data from Chen et al. 2003). The  $[\text{Fe}/\text{H}]$  gradient from cepheid variables is shown as a filled star. Also included are the following young objects: OB stars in associations etc. from Daflon & Cunha (2004, thick cross) and HII regions (x sign). The dotted vertical line shows the adopted age of the galactic disk,  $t_G = 13.6$  Gyr, and the dashed line represents the time evolution of the  $[\text{Fe}/\text{H}]$  gradient according to the theoretical models of Hou et al. (2000).

## 6. Discussion

An inspection of the O/H and S/H gradients from planetary nebulae shown in Table 1 and the  $[\text{Fe}/\text{H}]$  gradients from open clusters (Table 2) confirms that the average gradients have been flattening out for the last approximately 8 Gyr. These results are better seen in Fig. 8, where we plot the  $[\text{Fe}/\text{H}]$  gradients (dex/kpc) as a function of time, adopting  $t_G = 13.6$  Gyr for the age of the galactic disk. The gradients from planetary nebulae, obtained after converting the O/H gradients as discussed in Sect. 2 are shown as filled squares, while those derived from S/H data are shown as filled triangles. The horizontal error bars reflect the total age span as given in Table 1, and the vertical error bars are the calculated uncertainties of the least squares fits, as given in Table 1. The open cluster results are shown as filled circles for the data by Friel et al. (2002), and as empty circles for the objects in the sample by Chen et al. (2003), adopting the same criterium for the error bars. The  $[\text{Fe}/\text{H}]$  gradient from cepheid variables is shown as a filled star. Also included are the following young objects: OB stars in associations etc. from Daflon & Cunha (2004, thick cross) and HII regions, as discussed in Sect. 5 (x sign). The dotted vertical line shows the adopted age of the galactic disk,  $t_G = 13.6$  Gyr, and the dashed line represents the time evolution of the  $[\text{Fe}/\text{H}]$  gradient according to the theoretical models of Hou et al. (2000), which are based on an inside-out scenario for the formation of the disk using metallicity-dependent yields.

It can be seen from Fig. 8 that the open cluster gradients agree very well with the gradients derived from planetary nebulae, in the sense that both indicate a time flattening of the gradients during the lifetimes of these objects, which is taken here as up to 8 Gyr. This conclusion holds in spite of the relatively large uncertainties involved in the age determinations, especially in the case of the planetary nebula progenitor stars.

Although the division of the PN and open clusters into different age groups is arbitrary, it can be seen from Figs. 1, 2 and 4 that the time variation of the gradients is not sensitive to the particular groups chosen, as long as the age groups contain a reasonably large fraction of the total sample.

The main uncertainty in the time variation of the gradients, as seen in Fig. 8 refers to the youngest open clusters, since, as mentioned, these objects are preferentially concentrated in the inner Galaxy, so that the obtained correlation is not as accurate as in the remaining cases. This may partially explain the very low gradient found in Group I of both the Friel et al. (2002) and Chen et al. (2003) samples. Therefore, the gradient derived from the cepheid variable stars plays a very important role for ages under 1 Gyr, since it is well defined, as we have mentioned in Sect. 4. As expected, this gradient is steeper than those of Group I open clusters, but it still clearly suggests some flattening in comparison with the older objects in Fig. 8. Also in the young object bracket, it is interesting to notice that both the OB stars of Daflon & Cunha (2004) and the HII regions discussed in Sect. 5 also show a very good agreement with the scenario displayed by the remaining objects, and are perfectly consistent with the observed flattening during the last approximately 8 Gyr.

It is not our purpose here to discuss the effects of the present results on existing models of the chemical evolution of the Galaxy, rather our aim is to provide observational constraints to these models. As an illustration, however, the observational data discussed here also show a good agreement with theoretical models by Hou et al. (2000), as indicated by the dashed curve of Fig. 8. Naturally, our results refer to the last approximately 8 Gyr, which is the limit of the oldest age bracket for which we could derive some information. Nothing can then be said regarding the first 5 to 6 Gyr of the Galaxy lifetime,

assuming a total age of  $t_G = 13.6$  Gyr, so that our results do not contradict models that start with a null gradient, which may then build up in a relatively short time.

The flattening rate of the [Fe/H] gradient is still uncertain, in view of the considerable error bars shown in Fig. 8, but from a simple analysis of all objects considered here, an average rate of about  $0.005$  to  $0.010$  dex  $\text{kpc}^{-1}$   $\text{Gyr}^{-1}$  can be obtained. This is similar to the earlier results by Maciel et al. (2003) and Chen et al. (2003) for planetary nebulae and open clusters, respectively. Although this value is clearly uncertain, it sets the order of magnitude for the last 8 Gyr approximately, or from the time when the Galaxy was 5 to 6 Gyr old to the present time.

*Acknowledgements.* We thank P. A. L. Ferreira, P. S. Ribeiro and M. M. M. Uchida for some helpful discussions. This work was partly supported by FAPESP, CNPq and CAPES. Observations at ESO/Chile were possible through the FAPESP grant 98/10138-8.

## References

- Afflerbach, A., Churchwell, E., & Werner, M. W. 1997, *ApJ*, 478, 190  
 Alibés, A., Labay, J., & Canal, R. 2001, *A&A*, 370, 1103  
 Allende-Prieto, C., Lambert, D. L., & Asplund, M. 2001, *ApJ*, 556, L63  
 Andrievsky, S. M., Bersier, D., Kovtyukh, V. V., et al. 2002b, *A&A*, 384, 140  
 Andrievsky, S. M., Kovtyukh, V. V., Luck, R. E., et al. 2002a, *A&A*, 381, 32  
 Andrievsky, S. M., Kovtyukh, V. V., Luck, R. E., et al. 2002c, *A&A*, 392, 491  
 Andrievsky, S. M., Luck, R. E., Martin, P., & Lépine, J. R. D. 2004 *A&A*, 413, 159  
 Asplund, M. 2003, *CNO in the Universe*, ed. C. Charbonnel, D. Schaerer, & G. Meynet (San Francisco: ASP), ASP Conf. Ser., 304, 275  
 Asplund, M., Grevesse, N., Sauval, A. J., Allende-Prieto, C., & Kiselman, D. 2004, *A&A*, 417, 751  
 Bahcall, J. N., & Piran, T. 1983, *ApJ*, 267, L77  
 Binney, J., & Merrifield, M. 1998, *Galactic Astronomy* (Princeton University Press)  
 Caputo, F., Marconi, M., Musella, I., & Pont, F. 2001, *A&A*, 372, 544  
 Chen, L., Hou, J. L., & Wang, J. J. 2003, *AJ*, 125, 1397  
 Chiappini, C., Matteucci, F., & Romano, D. 2001, *ApJ*, 554, 1044  
 Costa, R. D. D., Uchida, M. M. M., & Maciel, W. J. 2004, *A&A*, 423, 199  
 Cox, A. N. 2000, *Allen's Astrophysical Quantities*, 4th. Ed., AIP  
 Daflon, S., & Cunha, K. 2004, *ApJ*, in press [arXiv:astro-ph/0409084]  
 Deharveng, L., Peña, M., Caplan, J., & Costero, R. 2000, *MNRAS*, 311, 329  
 Dias, W. S., Alessi, B. S., Moitinho, A., & Lépine, J. R. D. 2002, *A&A*, 389, 871  
 Friel, E. D. 1995, *ARA&A*, 33, 381  
 Friel, E. D. 1999, *Ap&SS*, 265, 271  
 Friel, E. D., Janes, K. A., Tavares, M., et al. 2002, *AJ*, 124, 2693  
 Friel, E. D. 2005, *Chemical abundances and mixing in stars in the Milky Way and its satellites*, ESO Conference, ed. L. Pasquini, & S. Randich (Springer), in press  
 Groenewegen, M. A. T., Romaniello, M., Primas, F., & Mottini, M. 2004, *A&A*, 420, 655  
 Henry, R. B. C., & Worthey, G. 1999, *PASP*, 111, 919  
 Henry, R. B. C., Kwitter, K. B., & Balick, B. 2004, *AJ*, 127, 2284  
 Hou, J. L., Prantzos, N., & Boissier, S. 2000, *A&A*, 362, 921  
 Janes, K. A. 1979, *ApJS*, 39, 135  
 Köppen, J., Acker, A., & Stenholm, B. 1991, *A&A*, 248, 19  
 Luck, R. E., Gieren, W. P., Andrievsky, S. M., et al. 2003, *A&A*, 401, 939  
 Maciel, W. J. 1993, *A&SS*, 206, 285  
 Maciel, W. J. 2000, in *The Evolution of the Milky Way*, ed. F. Matteucci, & F. Giovannelli (Dordrecht: Kluwer), 81  
 Maciel, W. J. 2002, *Rev. Mex. AA - SC*, 12, 207  
 Maciel, W. J., & Costa, R. D. D. 2003, *Planetary Nebulae*, ed. S. Kwok, M. Dopita, & R. Sutherland (San Francisco: ASP), IAU Symp., 209, 551  
 Maciel, W. J., Costa, R. D. D., & Uchida, M. M. M. 2003, *A&A*, 397, 667 (Paper I)  
 Maciel, W. J., & Köppen, J. 1994, *A&A*, 282, 436  
 Maciel, W. J., & Quireza, C. 1999, *A&A*, 345, 629  
 McNamara, D. H., Madsen, J. B., Barnes, J., & Ericksen, B. F. 2000, *PASP*, 112, 202  
 Phelps, R. 2000, in *The Evolution of the Milky Way*, ed. F. Matteucci, & F. Giovannelli (Dordrecht: Kluwer), 239  
 Pilyugin, L. S., Ferrini, F., & Shkvarun, R. V. 2003, *A&A*, 401, 557  
 Reid, M. J. 1993, *ARA&A*, 31, 345  
 Salaris, M., Weiss, A., & Percival, S. M. 2004, *A&A*, 414, 163  
 Smartt, S. J. 2000, in *The Evolution of the Milky Way*, ed. F. Matteucci, & F. Giovannelli (Dordrecht: Kluwer), 323  
 Tosi, M. 2000, in *The Evolution of the Milky Way*, ed. F. Matteucci, & F. Giovannelli (Dordrecht: Kluwer), 505  
 Twarog, B. A., Ashman, K. M., & Anthony-Twarog, B. J. 1997, *AJ*, 114, 2556  
 Vílchez, J. M., & Esteban, C. 1996, *MNRAS*, 280, 720